Simplification Operators on a Dimension-Independent Graph-Based Representation of Morse Complexes

Lidija Čomić[1], Leila De Floriani[2], and Federico Iuricich[2]

[1] University of Novi Sad - Faculty of Technical Sciences
comic@uns.ac.rs
[2] University of Genova - Department of Computer Science
deflo@disi.unige.it
federico.iuricich@unige.it

Abstract. Ascending and descending Morse complexes are defined by the critical points and integral lines of a scalar field f defined on a manifold M. They induce a subdivision of M into regions of uniform gradient flow, thus providing a compact description of the topology of M and of the behavior of f over M. We represent the ascending and descending Morse complexes of f as a graph, that we call the *Morse incidence graph (MIG)*. We have defined a simplification operator on the graph-based representation, which is atomic and dimension-independent, and we compare this operator with a previous approach to the simplification of 3D Morse complexes based on the cancellation operator. We have developed a simplification algorithm based on a simplification operator, which operates on the MIG, and we show results from this implementation as well as comparisons with the cancellation operator in 3D.

Keywords: geometric modeling, Morse theory, Morse complexes, simplification.

1 Introduction

Representing topological information extracted from discrete scalar fields is a relevant issue in several applications, such as terrain modeling, or analysis and visualization of static and time-varying 3D scalar fields arising from physical simulation or describing medical data. Morse theory offers a natural and intuitive way of analyzing the structure of a scalar field f as well as of compactly representing it through decompositions of its domain M into meaningful regions associated with the critical points of f, giving rise to the *Morse* and *Morse–Smale complexes*. *Descending* and *ascending* Morse complexes decompose M into cells defined by the integral lines of f converging to and originating at critical points of f, respectively. The Morse–Smale complex decomposes M into cells defined by integral lines with the same origin and destination. We represent here the topology of the descending and ascending Morse complexes in arbitrary dimensions as a graph, that we call the *Morse Incidence Graph* (MIG), in which the

C.L. Luengo Hendriks, G. Borgefors, R. Strand (Eds.): ISMM 2013, LNCS 7883, pp. 13–24, 2013.

nodes encode the cells of the Morse complexes, and the arcs encode their mutual incidence relations. The MIG provides also a combinatorial description of the Morse–Smale complex.

The main issue in the usage of Morse and Morse–Smale complexes in real-world applications scenarios lies in their storage requirements and computation costs when extracted from very large data sets describing 2D and 3D scalar fields, which are common in current applications. Thus, simplification of such complexes by reducing the number of cells and their mutual relations becomes a must. A separate, but still related, issue is the presence of noise in the data, which leads to over-segmentation. In this case as well, we need operators for simplifying Morse and Morse–Smale complexes and their combinatorial representation.

There have been two approaches in the literature to the simplification of Morse and Morse–Smale complexes. The approach in [13] is specific for 3D Morse–Smale complexes and is based on the cancellation operator defined in Morse theory [15]. The major problem with using cancellation is that it may increase the size of the Morse–Smale complexes when the cancellation does not involve a minimum or a maximum, thus causing memory problems when dealing with large-size data sets [11]. The approach in [4,5] is based on an atomic simplification operator, called *remove*, which is entirely dimension-independent, never increases the size of the complexes, and defines a minimally complete basis for expressing any simplification operator on such complexes.

Here, we report the effect of *remove* operator on the MIG. We show that its effect on the MIG is always local, and this is true in any dimension. Moreover, it is simple to implement in a completely dimension-independent way. We have also implemented the cancellation operator on the MIG in the 3D case and compared it with the 3D instances of the *remove* operator. We show that the size of the simplified MIG produced by *remove* is always smaller than that of the graph produced by cancellation.

The remainder of this paper is organized as follows. In Section 2, we review some basic notions on Morse theory and Morse complexes, some algorithms for their computation, and the relation between Morse complexes and the watershed decomposition. In Section 3, we describe a dual incidence-based graph representation of the Morse complexes, the *Morse Incidence Graph* (MIG). In Section 4, we recall the definition of the *remove* operator on the scalar field and we describe its effect on the MIG. In Section 5, we describe the effect of the cancellation operator in [13] on the MIG. In Section 6, we present experimental results on the behavior of the simplification algorithm based on *remove* and on the cancellation operators, and comparisons between our simplification operator and cancellation in 3D. Finally, in Section 7, we make some concluding remarks.

2 Background Notions and Related Work

Morse theory [15] captures the relation between the topology of a manifold M and the critical points of a scalar (real-valued) function f defined on M.

Let f be a C^2 real-valued function defined over a closed compact n-manifold M. A point p is a *critical point* of f if and only if the gradient $\nabla f = (\frac{\partial f}{\partial x_1}, ..., \frac{\partial f}{\partial x_n})$

(in some local coordinate system around p) of f vanishes at p. A function f is a *Morse function* if and only if all its critical points are non-degenerate (i.e., the Hessian matrix $Hess_p f$ of the second derivatives of f at a point p is non-singular). The number i of negative eigenvalues of $Hess_p f$ at p is called the *index* of p, and p is called an *i-saddle*. A 0-saddle is also called a *(local) minimum*, and an n-saddle a *(local) maximum*. An *integral line* of f is a maximal path which is everywhere tangent to ∇f. Each integral line starts and ends at critical points of f, called its *origin* and its *destination*.

Integral lines that converge to a critical point p of index i form an i-cell called a *descending cell*, or *manifold*, of p. Dually, integral lines that originate at p form its ascending $(n-i)$-cell. The descending and ascending cells decompose M into *descending* and *ascending Morse complexes*, denoted as Γ_d and Γ_a, respectively (see Figure 1 (a) and (b)). A Morse function f is called a *Morse–Smale function* if and only if each non-empty intersection of a descending and an ascending manifold is transversal. The connected components of the intersection define a *Morse–Smale complex* (see Figure 1 (c)).

The decomposition into ascending Morse complexes in 2D is related to the watershed decomposition, developed for image analysis. If f is a function which has a gradient ∇f everywhere except possibly at some isolated points, then the *topographic distance* $T_D(p,q)$ between two points p, q belonging to the domain D of f is defined as $T_D(p,q) = \inf_P \int_P |\nabla f(P(s))| ds$ [16,18]. If there is an integral line which reaches both p and q, then the topographic distance between these two points is equal to the difference in elevation between them. Otherwise, it is strictly greater than the difference in elevation. The *catchment basin* $CB(m_i)$ of a minimum m_i is the set of points which are closer (in the sense of topographic distance) to m_i than to any other minimum. The *watershed* $WS(f)$ of f is the set of points which do not belong to any catchment basin. When f is a Morse function, then the catchment basins of the minima of f correspond to the 2-cells in the ascending Morse complex of f.

Topological watershed [1] is obtained by lowering (until idempotence) some points of the original image while preserving the connectivity of each lower cross-section. This operator does not preserve the connected components or holes in a 3D object. The catchment basins and the watershed separating them are composed of pixels (2-cells) in the image, while in the ascending Morse complexes ascending 2-cells (corresponding to minima) are separated by 1-cells (corresponding to saddles).

Algorithms for decomposing the domain M of f into an approximation of a Morse, or of a Morse–Smale complex in 2D can be classified as *boundary-based* or *region-based*. In [7,6,14], algorithms for extracting the Morse–Smale complex from a tetrahedral mesh have been proposed. Discrete methods rooted in the discrete Morse theory proposed by Forman [9] are computationally more efficient [10,17]. For a survey, see [2,3]. Alternative region-based techniques for computing the ascending and descending Morse complexes are based on the discrete watershed transform (see [18] for a survey).

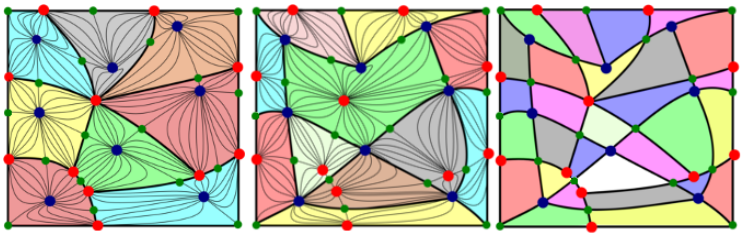

(a) (b) (c)

Fig. 1. A portion of an ascending Morse complex in 2D (a); the dual descending Morse complex (b); the corresponding Morse–Smale complex (c).

3 The Morse Incidence Graph (*MIG*)

The topology of complexes Γ_a and Γ_d is represented in the form of a graph, called the *Morse Incidence Graph (MIG)* $G = (N, A, \psi)$, where N is the set of nodes, A is the set of arcs, and $\psi : A \to \mathbb{N}$ is a labeling function, such that:

1. the set N of nodes is partitioned into $n+1$ subsets N_0, N_1,...,N_n, such that there is a one-to-one correspondence between the nodes in N_i (which we call *i-nodes*) and the i-cells of Γ_d, (and thus the $(n-i)$-cells of Γ_a);
2. there is an arc (p, q) joining an i-node p with an $(i+1)$-node q if and only if i-cell p is on the boundary of $(i+1)$-cell q in Γ_d, (and thus q is on the boundary of p in Γ_a);
3. each arc (p, q) is labeled with the number $\psi(p, q)$ of times i-cell p (corresponding to i-node p) in Γ_d is incident into $(i+1)$-cell q (corresponding to $(i+1)$-node q) in Γ_d, and thus $\psi(p, q)$ is equal to the number of integral lines of f connecting i-saddle p to $(i+1)$-saddle q.

Each node is labeled with the critical point (or equivalently, the descending cell) it represents. If f is a Morse–Smale function, then the MIG provides also a combinatorial representation of the 1-skeleton of its Morse–Smale complex. Figure 2 illustrates the descending and ascending complexes, and the corresponding MIG for function $f(x, y) = \cos x \cos y$.

4 The *Remove* Simplification Operator

In [4,5], we have introduced a dimension-independent simplification operator called *remove* on the Morse complexes and on the MIG representing them. This operator (together with its inverse one) forms a basis for defining any operator that updates Morse and Morse–Smale complexes on a manifold M in a topologically consistent manner. Operator *remove* has two instances, namely $remove_{i,i+1}$ and $remove_{i,i-1}$, for $1 \leq i \leq n-1$. We describe the effect of the *remove* operator on the Morse function f and on the corresponding MIG.

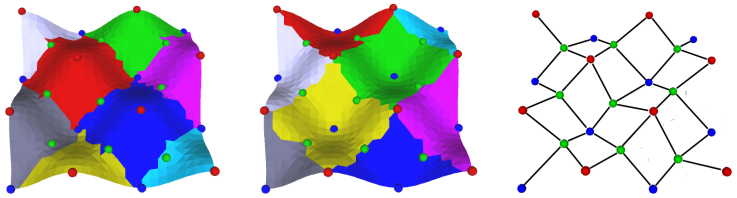

(a) (b) (c)

Fig. 2. The descending (a) and ascending (b) 2D Morse complex for function $f(x, y) = \cos x \cos y$ and the corresponding MIG (c).

4.1 *Remove* on the Scalar Field

A $remove_{i,i+1}$ operator collapses an i-saddle q and an $(i+1)$-saddle p, that are connected through a unique integral line. It is defined if i-saddle q is connected to at most one other $(i+1)$-saddle p' different from $(i+1)$-saddle p. There are two types of $remove_{i,i+1}$, denoted as $remove_{i,i+1}(q, p, p')$ and $remove_{i,i+1}(q, p, \emptyset)$, respectively. $Remove_{i,i+1}(q, p, p')$ applies when the i-saddle q is connected to the $(i+1)$-saddle p and exactly one other $(i+1)$-saddle p' different from p. It collapses the i-saddle q and the $(i+1)$-saddle p into the $(i+1)$-saddle p'. $Remove_{i,i+1}(q, p, \emptyset)$ deals with the situation in which the i-saddle q is connected to only one $(i+1)$-saddle p. It eliminates the i-saddle q and the $(i+1)$-saddle p from the set of critical points of the scalar field f.

$Remove_{i,i-1}(q, p, p')$ operator is dual to the previous one. It collapses an i-saddle q and an $(i-1)$-saddle p that are connected through a unique integral line. As for $remove_{i,i+1}$, there are two types of $remove_{i,i-1}$ operator, denoted as $remove_{i,i-1}(q, p, p')$ and $remove_{i,i-1}(q, p, \emptyset)$, respectively. $Remove_{i,i-1}(q, p, p')$ applies when the i-saddle q is connected to the $(i-1)$-saddle p and exactly one other $(i-1)$-saddle p' different from p. It collapses the i-saddle q and $(i-1)$-saddle p into the $(i-1)$-saddle p'. $Remove_{i,i-1}(q, p, \emptyset)$ eliminates the i-saddle q and the unique $(i-1)$-saddle p connected to q.

In 2D, we have two *remove* operators, both deleting a saddle and an extremum. $Remove_{1,2}(q, p, p')$ consists of collapsing a maximum (2-saddle) p and a saddle (1-saddle) q into a maximum (2-saddle) p', and $remove_{1,0}(q, p, p')$ consists of collapsing a minimum (0-saddle) p and a saddle (1-saddle) q into a minimum (0-saddle) p'. $Remove_{1,2}(q, p, \emptyset)$ consists of deleting a maximum (2-saddle) p and a saddle (1-saddle) q. Dually, $remove_{1,0}(q, p, \emptyset)$, consists of deleting a minimum (0-saddle) p and a saddle (1-saddle) q.

In 3D there are four *remove* operators, two $remove_{i,i+1}$ and two $remove_{i,i-1}$ operators. $Remove_{2,3}(q, p, p')$ collapses a maximum (3-saddle) p and a 2-saddle q into a maximum (3-saddle) p', while $remove_{1,2}(q, p, p')$, collapses a 2-saddle p and a 1-saddle q into a 2-saddle p'. Dually, $remove_{1,0}(q, p, p')$ collapses a minimum (0-saddle) p and a 1-saddle q into a minimum (0-saddle) p', while $remove_{2,1}(q, p, p')$ collapses a 1-saddle p and a 2-saddle q into a 1-saddle p'. The operators of the second type delete the two critical points q and p.

4.2 *Remove* on the *MIG*

On a $MIG\ G = (N, A, \psi)$, the effect of the *remove* operator is to transform G into a simplified $MIG\ G' = (N', A', \psi')$ by eliminating two nodes p and q from N, and reconnecting the remaining nodes in the simplified graph G' so that $|N'| = |N| - 2$ and $|A'| < |A|$. Let us consider the effect of $remove_{i,i+1}(q, p, p')$. We consider the following sets of nodes in the $MIG\ G = (N, A, \psi)$:

- $Z = \{z_h, h = 1, .., h_{max}\}$ is the set of the $(i-1)$-nodes connected to the i-node q;
- $S = \{s_k, k = 1, .., k_{max}\}$ is the set of the $(i+2)$-nodes connected to the $(i+1)$-node p;
- $R = \{r_j, j = 1, .., j_{max}\}$ is the set of the i-nodes connected to the $(i+1)$-node p (the set R may be empty).

The set S is empty for $i = n - 1$. For $remove_{i,i+1}(q, p, \emptyset)$ operator, the sets Z, R and S are exactly the same as for $remove_{i,i+1}(q, p, p')$.

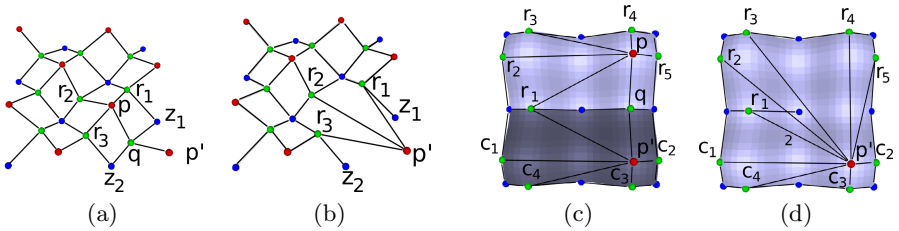

Fig. 3. An example of a $remove_{1,2}(q, p, p')$ on a MIG in the 2D case (a) and (b). MIG overlayed on the descending Morse complex before (c) and after (d) $remove_{1,2}(q, p, p')$ in 2D. The label of the arc connecting nodes r_1 and p' is increased to 2, and 1-cell r_1 appears two times on the boundary of 2-cell p' after $remove_{1,2}(q, p, p')$.

Figure 3 (a) illustrates $remove_{1,2}(q, p, p')$ in 2D, which is a maximum-saddle operator. The set Z consists of nodes z_1 and z_2, which correspond to minima. The set S is empty since the operator involves an extremum. The set R consists of saddles r_1, r_2 and r_3 connected to the maximum p.

$Remove_{i,i+1}(q, p, p')$ operator is feasible on a $MIG\ G = (N, A, \psi)$ if

- i-node q is connected to exactly two different $(i+1)$-nodes p and p', and
- the label of arc (p, q) is 1 ($\psi(p, q) = 1$).

The effect of $remove_{i,i+1}(q, p, p')$ on G is to

- delete nodes p and q,
- delete all the arcs incident in either i-node q or $(i+1)$-node p,
- introduce an arc (p, r_j) for each $r_j \in R$ (if such arc does not already exist),
- set $\psi'(p', r_j) = \psi(p', q) \cdot \psi(p, r_j) + \psi(p', r_j)$.

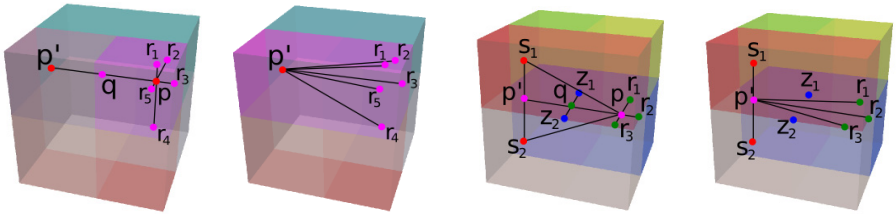

(a) (b) (c) (d)

Fig. 4. The MIG, overlayed on the descending Morse complex, before (a) and after (b) $remove_{2,3}(q, p, p')$, and before (a) and after (b) $remove_{1,2}(q, p, p')$ in 3D.

The labels of other arcs in the simplified MIG $G' = (N', A', \psi')$ remain unchanged.

In the example illustrated in Figure 3 (a) and (b), $remove_{1,2}(q, p, p')$, deletes nodes p and q, as well as the arcs incident in 1-node q (arcs (q, p), (q, p'), (q, z_1) and (q, z_2)). Arcs (p, r_1), (p, r_2) and (p, r_3) are replaced with arcs (p', r_1), (p', r_2) and (p', r_3).

Figure 3 (c) and (d) illustrates the effect of $remove_{1,2}(q, p, p')$ in 2D, which is a saddle-maximum removal. Before $remove_{1,2}(q, p, p')$, 1-node r_1 is connected to 2-nodes p and p', and the labels of arcs (p, r_1) and (p', r_1) are equal to 1 ($\psi(p, r_1) = \psi(p', r_1) = 1$). After $remove_{1,2}(q, p, p')$, the label of arc (p', r_1) is equal to 2 ($\psi'(p', r_1) = \psi(p', q) \cdot \psi(p, r_1) + \psi(p', r_1) = 1 \cdot 1 + 1 = 2$). The labels of other arcs in the graph are equal to 1.

Figure 4 (a) and (b) illustrates the effect of $remove_{2,3}(q, p, p')$ in 3D, which performs the removal of a 2-saddle and a maximum. Nodes p and q are deleted as well as all the arcs incident in 2-node q. Arcs (p, r_1), (p, r_2), (p, r_3), (p, r_4) and (p, r_5) are replaced with arcs (p', r_1), (p', r_2), (p', r_3), (p', r_4) and (p', r_5).

Figure 4 (c) and (d) shows the effect of $remove_{1,2}(q, p, p')$ in 3D, which is a 1-saddle-2-saddle removal. Nodes p and q are deleted, as well as all the arcs incident in 1-node q, and arcs connecting 2-node p to 3-nodes s_1 and s_2. Arcs (p, r_1), (p, r_2) and (p, r_3) are replaced with arcs (p', r_1), (p', r_2) and (p', r_3). The dual $remove_{i,i-1}(q, p, p')$ operator can be expressed as a modification of the graph $G = (N, A, \psi)$ in a completely dual fashion.

5 Operator *i-Cancellation*

The cancellation operator [13], that we call *i-cancellation*, is a simplification operator defined in Morse theory [15]. It eliminates i-saddle q and $(i+1)$-saddle p connected through a unique integral line, but it does not impose any constraints on the number of $(i+1)$-saddles connected to q, or on the number of i-saddles connected to p. We define here the *i-cancellation*(q, p) operator on the MIG. We denote as $T = \{t_l, l = 1, ..., l_{max}\}$ the set of $(i+1)$-nodes different from $(i+1)$-node p and connected to i-node q. $R = \{r_j, j = 1, .., j_{max}\}$ is the set of i-nodes (i-saddles) connected to p and different from q.

An *i-cancellation*(q, p), $0 \leq i \leq n-1$, is feasible on a MIG $G = (N, A, \psi)$ if

- i-node q is connected to $(i+1)$-node p, and
- the label of arc (p, q) is 1 ($\psi(p, q) = 1$).

The effect of *i-cancellation*(q, p) is to

- delete i-node q and $(i+1)$-node p,
- delete all the arcs incident in either i-node q or $(i+1)$-node p,
- introduce an arc (t_l, r_j) for each $t_l \in T$ and each $r_j \in R$ (if such arc does not already exist),
- set $\psi'(t_l, r_j) = \psi(t_l, q) \cdot \psi(p, r_j) + \psi(t_l, r_j)$.

The labels of the other arcs in the simplified MIG $G' = (N', A', \psi')$ are the same as the labels of those arcs in G.

In the 2D case, $remove_{1,2}(q, p, p')$ is the same as the maximum-saddle 1-*cancellation*(q, p), and $remove_{1,0}(q, p, p')$ is the same as the minimum-saddle 0-*cancellation*(p, q). In 3D, $remove_{2,3}(q, p, p')$ operator involving an extremum (maximum-2-saddle) is exactly the same as the 2-*cancellation*(q, p). Dually, $remove_{1,0}(q, p, p')$ operator involving an extremum (minimum-1-saddle) is exactly the same as the 0-*cancellation*(p, q). In general, $remove_{n-1,n}(q, p, p')$ and $remove_{1,0}(q, p, p')$ operators involving an extremum p are the same as the $(n-1)$-*cancellation*(q, p) and 0-*cancellation*(p, q), respectively.

The *i-cancellation* involving only saddles (which are not extrema) is more complex. As an example, let us consider the 1-*cancellation* of a 1-saddle and a 2-saddle in 3D. This operator has been implemented in [12,11] on the 1-skeleton of the Morse–Smale complex (which is combinatorially equivalent to the MIG of the corresponding Morse complexes). The 1-*cancellation*(q, p) of 1-node q and 2-node p is feasible on the MIG $G = (N, A, \psi)$ if nodes q and p are connected, and the label of arc (p, q) is 1 ($\psi(p, q) = 1$). Let $G' = (N', A', \psi')$ be the graph after 1-*cancellation*(q, p). The effect of 1-*cancellation*(q, p) consists of deleting nodes p and q, as well as all the arcs incident in nodes p and q, and adding one arc for each pair (r_j, t_l) where r_j belongs to R and t_l belongs to T. Thus, the 1-*cancellation* operator deletes two nodes from N, but it increases the number of arcs connecting 1-nodes to 2-nodes in the graph by deleting $|R| + |T| + 1$ of such arcs, but adding $|R| * |T|$ of them. Thus, it is not a simplification operator, since it does not reduce the size of the graph. In [11], this issue has been discussed at length, since it can cause computational problems and, more importantly, make the application of *i-cancellation* operator unfeasible on large-scale data sets. Several strategies are proposed in [11], which aim at postponing an *i-cancellation* that would introduce a number of arcs greater than a predefined threshold, or vertices with valence greater than a predefined threshold. On the contrary, the *remove* operator always reduces the size of the graph.

6 Experimental Results

We have performed experiments on the simplification of Morse complexes by using six data sets describing 2D scalar fields, and eight data sets describing 3D

Table 1. Comparison of *cancellation* and *remove* operators

Name	N Simpl	Nodes	Arcs	Cost (MB)	Time (sec.)
Neghip		3K	11512	0.17	-
i-cancellation	1200	700	2621	0.04	0.68
remove	1200	700	2395	0.03	0.62
Hydrogen	-	23K	65961	1.0	-
i-cancellation	7000	9K	35123	0.53	25.1
remove	7000	9K	23091	0.35	17.86
Bucky	-	46K	157984	2.4	-
i-cancellation	7000	32K	128231	1.95	73.5
remove	7000	32K	84487	1.23	33.4
Aneurism	-	125K	1015724	15.49	-
i-cancellation	10000	105K	748192	11.41	233.28
remove	10000	105K	435910	6.65	70.54
VisMale	-	900K	3588570	54.75	-
i-cancellation	10000	880K	3513889	53.61	37.12
remove	10000	880K	3107124	47.41	9.43
Foot	-	1550K	7178384	109.5	-
i-cancellation	45000	1460K	6137199	93.64	2882.1
remove	45000	1460K	5413683	82.6	1187.3

scalar fields on a 3.2GHz processor with 2.0Gb memory. The MIG representing the Morse complexes is extracted using the algorithm described in [17].

We have developed a simplification algorithm for Morse complexes in arbitrary dimensions based on the $remove_{i,i+1}$ and $remove_{i,i-1}$. A *persistence* value is associated with any *remove* operator by considering the function values of the two critical points p and q deleted by the operator. Intuitively, the *persistence* of a pair of critical points measures the importance of the pair and is equal to the absolute difference in function values between the two points [8]. The objective of the simplification algorithm is to reduce the size of the Morse complex by removing critical points which are due to the presence of noise or which are not relevant for the need of a specific application. Simplification is also applied when the size of the original Morse complex is too large for the computation resources available.

The simplification algorithm starts by computing all feasible simplifications, evaluates their persistence and inserts them in an ordered queue in increasing order of persistence. At each step, a simplification is removed from the queue and applied to the current MIG. The process terminates when either a certain number of simplifications has been performed or when a specified value of persistence is reached.

We have also implemented a 3D version of the simplification algorithm based on cancellation. In this case, the number of critical nodes is reduced at each step, but not necessarily the number of arcs.

In the experiments, we have used different thresholds on persistence value: 1% of the max persistence value for light noise removal, 10% for stronger noise removal, and 20% or greater for consistently reducing the complexity of the

MIG. The storage cost of the simplified MIG using these three different thresholds is equal to 95%, 65% and 35% of the cost of the MIG at full resolution.

We have also analyzed the statistics on the operators involved in the simplification process for some 3D data sets. We have noticed that saddle-saddle simplification operators are likely to be performed early in the simplification process. If the simplification algorithm is based on persistence, this means that a large number of arcs will be introduced in the MIG early in the simplification process, influencing both the efficiency (speed) of the algorithm and its versatility (the number of feasible simplifications). This result underlines the importance of having an efficient operator for simplifying saddles.

In Table 1, we show the results obtained by comparing the *remove* operator with the *cancellation* operator. For each 3D data set, we show in the first row the number of nodes and arcs in the full resolution MIG. In the second and third rows, we show the statistics related to *cancellation* and *remove* operators, respectively: the number of simplifications applied, the number of nodes and arcs in the simplified MIG, the cost of the data structure encoding the MIG (in MB), and the time (in sec) needed to perform the simplifications.

The number of arcs in the graph simplified with *cancellation* always exceeds the number of arcs in the graph simplified with the same number of *remove*. Such behavior influences the efficiency of the whole algorithm, doubling the time needed to manage and enqueue a larger number of arcs (and thus, a greater number of possible simplifications) for large data sets.

When the data set is small and the number of simplifications is high compared to the total number of nodes the two methods are quite similar ($Neghip$). With the growth of the dimension of the data set the two methods start to differ ($Hydrogen$): by using *remove* we can get a 20% more compressed MIG in about half the time than by using *cancellation*. In particular, the *remove* operator is particularly useful in the first simplifications performed on a data set (simplifications that can be interpreted as noise removal). On many data sets we have noticed that by using *cancellation* the number of arcs remains approximately the same while by using *remove* their number immediately decreases ($VisMale$). In general, the cost of the MIG is reduced by 10% to 20% by using *remove* instead of *cancellation* and the same number of simplifications can be performed in half the time.

In Figure 5, we illustrate the result of our simplification algorithm on a 3D *Buckyball* data set (Figure 5 (a)), which represents the electron density inside a C-60 Buckminsterfullerene. The full-resolution MIG is shown in Figure 5 (b). The MIGs after 11K and 12K simplifications are shown in Figure 5 (c) and (d), respectively.

7 Concluding Remarks

We have described two simplification operators on the MIG representing the topology of the Morse complexes of a scalar field f. The *remove* operator always reduces the size of the MIG, both in terms of the number of nodes and of the

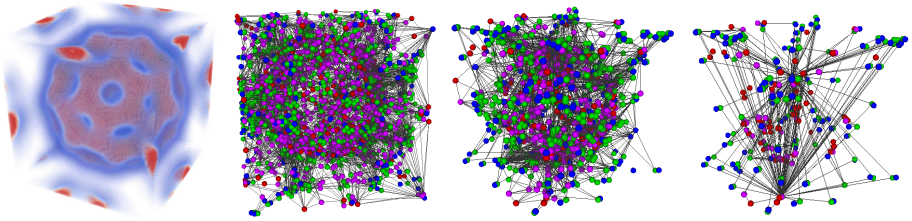

(a) (b) (c) (d)

Fig. 5. The field behavior for the *Buckyball* data set (a). The MIG at full resolution (b), the MIG after 11K (c) and after 12K simplifications (d).

number of arcs in the MIG. The *i-cancellation* operator is guaranteed to reduce only the number of nodes in the MIG, but in the general case it increases the number of its arcs, thus increasing the total size of the MIG.

We have designed and implemented a simplification algorithm based on the two simplification operators on the MIG, and we have performed experiments to compare the two operators. We have shown that the number of arcs in the simplified MIG obtained through the *i-cancellation* operator always exceeds the number of arcs in the simplified MIG obtained through the *remove* operator. The large number of arcs in the MIG influences not only the storage cost of the data structure for encoding it and the time required for performing the simplifications, but it also reduces the number of feasible simplification and thus the flexibility of the simplification algorithm.

Based on the *remove* operator, we have designed and implemented a multi-resolution model for the Morse complexes represented as a MIG that we call the *Multi-Resolution Morse Incidence Graph (MMIG)* [5]. It encodes a large number of topological representations of the Morse complexes at both uniform and variable level of detail.

Acknowledgments. This work has been partially supported by the Italian Ministry of Education and Research under the PRIN 2009 program, and by the National Science Foundation under grant number IIS-1116747.

References

1. Bertrand, G.: On Topological Watersheds. Journal of Mathematical Imaging and Vision 22(2-3), 217–230 (2005)
2. Biasotti, S., De Floriani, L., Falcidieno, B., Papaleo, L.: Morphological Representations of Scalar Fields. In: De Floriani, L., Spagnuolo, M. (eds.) Shape Analysis and Structuring, pp. 185–213. Springer (2008)
3. Biasotti, S., Floriani, L.D., Falcidieno, B., Frosini, P., Giorgi, D., Landi, C., Papaleo, L., Spagnuolo, M.: Describing shapes by geometrical-topological properties of real functions. ACM Comput. Surv. 40, Article 12 (2008)

4. Čomić, L., De Floriani, L., Iuricich, F.: Simplifying Morphological Representations of 2D and 3D Scalar Fields. In: 19th ACM SIGSPATIAL International Symposium on Advances in Geographic Information Systems, ACM-GIS 2011, pp. 437–440. ACM (2011)
5. Čomić, L., De Floriani, L., Iuricich, F.: Dimension-Independent Multi-Resolution Morse Complexes. Computers & Graphics 36(5), 541–547 (2012)
6. Edelsbrunner, H., Harer, J.: The Persistent Morse Complex Segmentation of a 3-Manifold. In: Magnenat-Thalmann, N. (ed.) 3DPH 2009. LNCS, vol. 5903, pp. 36–50. Springer, Heidelberg (2009)
7. Edelsbrunner, H., Harer, J., Natarajan, V., Pascucci, V.: Morse-Smale Complexes for Piecewise Linear 3-Manifolds. In: Proceedings 19th ACM Symposium on Computational Geometry, pp. 361–370 (2003)
8. Edelsbrunner, H., Harer, J., Zomorodian, A.: Hierarchical Morse Complexes for Piecewise Linear 2-Manifolds. In: Proceedings 17th ACM Symposium on Computational Geometry, pp. 70–79 (2001)
9. Forman, R.: Morse Theory for Cell Complexes. Advances in Mathematics 134, 90–145 (1998)
10. Gyulassy, A., Bremer, P.-T., Hamann, B., Pascucci, V.: A Practical Approach to Morse-Smale Complex Computation: Scalability and Generality. IEEE Transactions on Visualization and Computer Graphics 14(6), 1619–1626 (2008)
11. Gyulassy, A., Bremer, P.-T., Hamann, B., Pascucci, V.: Practical Considerations in Morse-Smale Complex Computation. In: Topological Methods in Data Analysis and Visualization: Theory, Algorithms, and Applications. Mathematics and Visualization, pp. 67–78. Springer (2011)
12. Gyulassy, A., Natarajan, V., Pascucci, V., Bremer, P.-T., Hamann, B.: Topology-Based Simplification for Feature Extraction from 3D Scalar Fields. In: Proceedings IEEE Visualization 2005, pp. 275–280. ACM Press (2005)
13. Gyulassy, A., Natarajan, V., Pascucci, V., Bremer, P.-T., Hamann, B.: A Topological Approach to Simplification of Three-Dimensional Scalar Functions. IEEE Transactions on Visualization and Computer Graphics 12(4), 474–484 (2006)
14. Gyulassy, A., Natarajan, V., Pascucci, V., Hamann, B.: Efficient Computation of Morse-Smale Complexes for Three-dimensional Scalar Functions. IEEE Transactions on Visualization and Computer Graphics 13(6), 1440–1447 (2007)
15. Matsumoto, Y.: An Introduction to Morse Theory. Translations of Mathematical Monographs, vol. 208. American Mathematical Society (2002)
16. Meyer, F.: Topographic distance and watershed lines. Signal Processing 38, 113–125 (1994)
17. Robins, V., Wood, P.J., Sheppard, A.P.: Theory and Algorithms for Constructing Discrete Morse Complexes from Grayscale Digital Images. IEEE Trans. Pattern Anal. Mach. Intell. 33(8), 1646–1658 (2011)
18. Roerdink, J., Meijster, A.: The Watershed Transform: Definitions, Algorithms, and Parallelization Strategies. Fundamenta Informaticae 41, 187–228 (2000)